nature catalysis

ANALYSIS

https://doi.org/10.1038/s41929-020-00527-4

Check for updates

Revealing nitrogen-containing species in commercial catalysts used for ammonia electrosynthesis

Yifu Chen[1], Hengzhou Liu[1], Nguon Ha[2], Stuart Licht[3]✉, Shuang Gu[2]✉ and Wenzhen Li[1,4]✉

Stimulated by the growing demand for sustainable and/or economical distributed ammonia synthesis, the electrochemical nitrogen reduction reaction has attracted considerable interest. The nitrogen-containing impurities in commercial metal-based nitrogen reduction reaction catalysts such as metal oxides and metallic irons have, however, been overlooked. Herein we report the presence of nitrogen-containing species in NO_x^- or nitrides at substantial levels revealed from many commercial catalysts. We call attention to the necessity to screen the NO_x^-/nitrides impurities in commercial catalysts, as the nitrogen impurities are not commonly listed in vendors' assay documents. A simple two-step procedure (alkaline/acidic treatment followed by HPLC/UV-vis analysis) is recommended as a reliable protocol for screening NO_x^-/nitrides impurities in catalyst materials. A case analysis is also carried out on the previously reported H_2O–NaOH–KOH system with both ^{15}N-isotopic labelling and nitrogen elemental tracking, reassigning the true nitrogen source of the electrochemically produced NH_3 from gaseous N_2 to nitrogen-containing impurities in catalysts.

With a century of optimization, the Haber–Bosch process has become the most successful procedure at fixing elemental N_2. About 180 million metric tons of artificial NH_3 is annually synthesized in centralized plants worldwide[1,2]—and with its widespread usage for fertilizers to increase crop yields, it is one of the greatest achievements of human civilization in the twentieth century. Due to the nature of N_2-fixing chemistry, the Haber–Bosch process demands not only harsh conditions for high reactivity (typically, 300–500 °C and 150–250 bar[3,4]) but also molecular H_2 as the key reactant along with N_2. In fact, the H_2 generation used for NH_3 synthesis heavily rests on the reforming of fossil fuels (dominantly, natural gas), using approximately 1% of global energy supply and contributing to 1–2% of total CO_2 emissions[3,5]. Furthermore, the essential requirements for harsh conditions as well as molecular H_2 pose great challenges for economically downscaling the process to distributed NH_3 production, which is preferred in remote areas or underdeveloped regions where transportation and storage are prohibitively costly[6,7]. Stimulated by the growing interest in exploring sustainable and/or economical distributed NH_3 synthesis, electrochemical and photochemical approaches have emerged as promising candidates.

The past few years have witnessed remarkable research activities into the electrocatalytic nitrogen reduction reaction (NRR) under desirably milder conditions[8,9], and metal-based materials (such as metal oxides and metal alloys) have been used as NRR catalysts with varying approaches. Yet, the true source of the produced NH_3 was recently appealed for by the research community[10–12], and a rigorous protocol with ^{15}N isotopic labelling was offered for careful examination[12]. Nitrogen leaching from certain NRR catalysts, such as metal nitrides, has been carefully studied[13–16] as elemental nitrogen is present in their known chemical compositions; however, the levels of the nitrogen-containing impurities in more general commercial catalysts used for NH_3 electrosynthesis have been overlooked, largely due to the long-built trust in the high quality of chemicals from mainstream chemical vendors.

In this work we selected a group of metal oxides and metallic iron for the focus of our analysis, in light of their frequent usage in the preparation of catalytic materials in different NRR systems[17–21]. The contents of nitrogen-containing impurities in their commercial products were carefully examined. Surprisingly, high levels of NO_3^- and NO_2^- ions were detected in some commercial oxides (for example, 1,610 ± 48 ppm of total NO_x^--N in one commercial Bi_2O_3 sample), and the content of nitrides-N in one commercial iron was as high as 7,297 ± 99 ppm. Various analytical techniques—including HPLC, UV, thermogravimetric analysis–mass spectrometry (TGA–MS), X-ray photoelectron spectroscopy (XPS), scanning electron microscopy–energy dispersive X-ray spectroscopy (SEM–EDS) and NMR—were utilized to validate the amount and nature of those nitrogen-containing species. Supported by our findings on the substantial levels of nitrogen-containing impurities in many commercial metal oxides, a case analysis was carried out on the previously reported H_2O–NaOH–KOH system[19] with both ^{15}N-isotopic labelling and nitrogen elemental tracking, reassigning the true reactant of putative NH_3 electrosynthesis from gaseous N_2 to nitrogen-containing impurities in the Fe_2O_3 catalyst.

Revealing unexpected NO_x^- impurities in commercial metal oxides

NO_x^- species ($x = 2$ or 3) are highly soluble in water and known to exist widely in nature. Here we first extracted both NO_2^- and NO_3^- by soaking the catalyst samples in an alkaline solution (0.1 M KOH) and then quantified them by analysing the soaking solution with an HPLC equipped with a UV detector (Figs. 1 and 2a, and Supplementary Fig. 2). The nitrogen content of NO_3^- in the commercial Fe_2O_3 (Alfa Aesar no. 45007) was determined to be 563 ± 21 ppm. In addition to the Fe_2O_3 (Alfa Aesar no. 45007), we

[1]Department of Chemical & Biological Engineering, Iowa State University, Ames, IA, USA. [2]Department of Mechanical Engineering, Wichita State University, Wichita, KS, USA. [3]Department of Chemistry, George Washington University, Washington, DC, USA. [4]DOE's Ames Laboratory, Ames, IA, USA. ✉e-mail: slicht@gwu.edu; shuang.gu@wichita.edu; wzli@iastate.edu

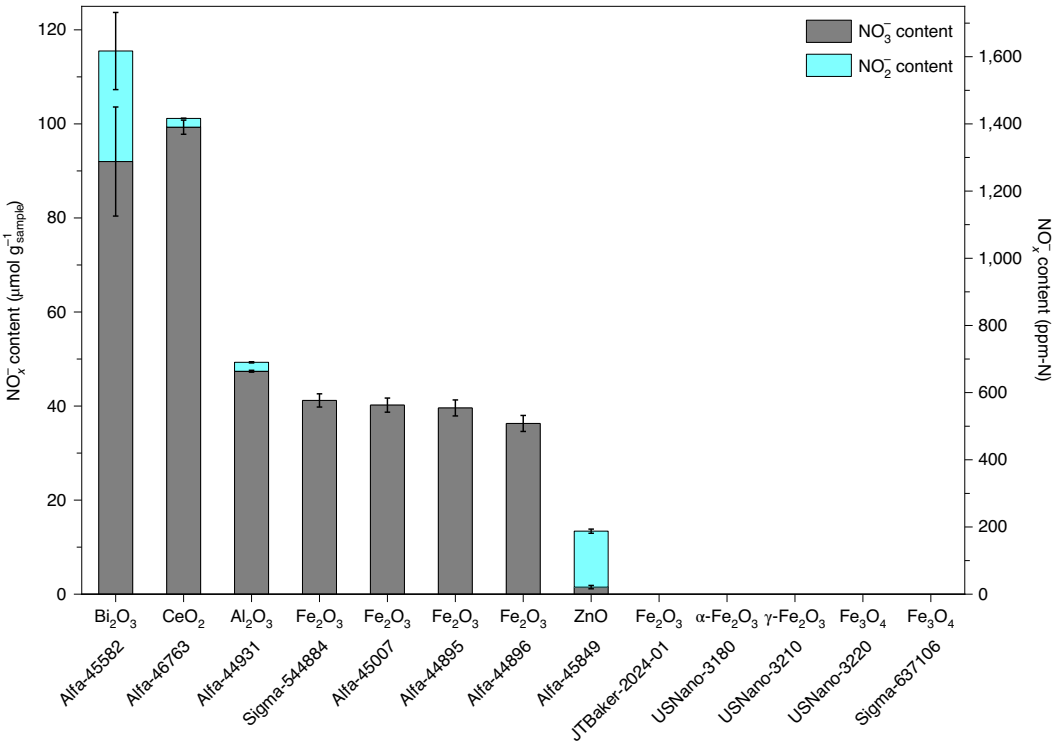

Fig. 1 | NO_x^- impurities detected in commercial metal oxides. The NO_x^- contents were determined by the two-step procedure (alkaline treatment followed by HPLC analysis). Briefly, the samples of commercial metal oxides were treated with an alkaline solution (0.1 M KOH) under ultrasonication for sufficient time. After treatment, the solids were filtered out and the remaining solutions were analysed by the calibrated HPLC for the contents of both NO_3^- and NO_2^- (see Methods). The error bars represent the standard deviation of NO_3^- and NO_2^- contents determined from three independent samples with the same lot number. The vendors, item numbers, lot numbers, labelled assays and values of NO_x^--N content of the tested samples are summarized in Supplementary Table 1.

further quantified the NO_x^- contents in another six commercial oxides from Alfa Aesar and six iron oxides from other vendors. The results, listed in Fig. 1, showed that 8 of 13 oxide samples contain appreciable levels of NO_3^- and/or NO_2^- impurities; it is quite unexpected to discover that such high levels of NO_x^- exist in those metal oxides. Note that aside from Fe_2O_3, other oxides such as Bi_2O_3 (ref. [17]), CeO_2 (ref. [18]) and ZnO (ref. [22]) are also included here as they have been actively involved in NH_3 electrosynthesis, although the commercial products were not used directly. The NO_3^- impurities in the iron oxides can be reduced by 99% via washing with 0.1 M KOH solution, or by 95% via a 12 h heat treatment at 180 °C (labelled as Fe_2O_3-washed and Fe_2O_3-HT, respectively).

In addition to the determined NO_x^- impurities from HPLC, we also directly observed NO—the signature product evolved during thermal decomposition of NO_3^-—from TGA–MS analysis (Fig. 2b). The NO signal ($m/z = 30$) appeared at ~150 °C, which is in good agreement with the decomposition temperature of metal nitrates[23,24].

In fact, the arc-discharging technique was employed to manufacture some commercial oxide products[25] (for example, some Alfa Aesar catalysts manufactured by NanoArc), which might explain the origin of the NO_x^- contamination that exists in a spectrum of oxides. After all, the use of non-catalytic electric arc had been proven effective at fixing N_2 oxidatively (that is, the Birkeland–Eyde process[26]) in the early twentieth century.

Revealing unexpected nitrides impurities in commercial metallic irons

Metallic iron is the precursor for industrial production of nanoscale Fe_2O_3 (ref. [25]) and a benchmark catalyst for heterogeneous N_2 fixation. Historically, the iron nitrides as impurities in metallic iron catalysts had confused some pioneered researchers in early N_2 fixation (that is, Wilhelm Ostwald in 1900[27]) even before the invention of the Haber–Bosch process. We cautiously examined the nitrogen impurities of five commercial iron products by dissolving them in 0.1 M H_2SO_4 (nitrides-N was hydrolysed to NH_4^+) and then determining the concentration of NH_4^+ in the resulting solution via the well-established indophenol blue colourimetric method[28]. As shown in Fig. 2c and Supplementary Fig. 3, NH_4^+-N was observed in all five iron sample solutions, presumably from nitrides. In particular, the iron product (Alfa Aesar no. 40337) contains 7,297 ± 99 ppm-N (or 3 at%), and the high level of nitrogen impurities was further verified in the quantitative NH_4^+ measurement by NMR (7.78×10^3 ppm). The other four commercial iron samples contain 300–400 ppm of nitrogen impurities, which is in strong contrast to the clean background (0.1 M H_2SO_4).

The presence of iron nitrides in iron samples is understandable because of the high chemical affinity between iron and nitrogen. In fact, chemisorption of nitrogen on metallic iron surfaces has been extensively studied in the past (that is, by Ertl and co-workers[29]) and the formation of surface nitrides was identified as a crucial step in heterogeneous N_2 fixation. It should be pointed out that the chemical composition of iron nitrides in those commercial iron products is not exactly the same from one to another. For example, the distinctive XPS nitrogen 1*s* signals were observed: 399.6 eV for Alfa Aesar-40337 (7,297 ppm-N) versus 403.5 eV for Sigma-Aldrich-255637 (391 ppm-N; Fig. 2d), that is, at values comparable with that of the bulk nitrides[30] (~397 eV). The difference in the position of the nitrogen 1*s* peak could probably be attributed to the different numbers of oxygen atoms linked to nitrogen[30,31], considering the identified XPS signals from nitrosonium (NO^+, 399–402 eV) and nitrite (NO_2^-,

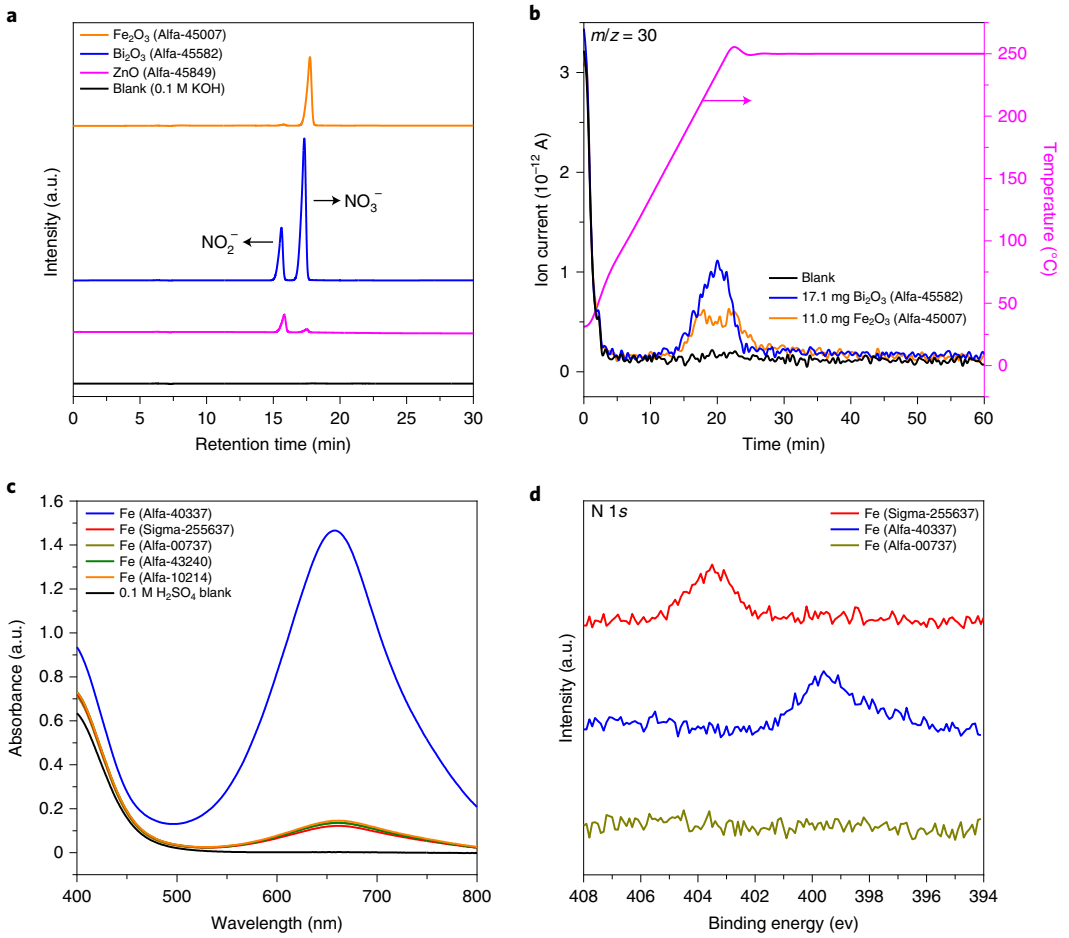

Fig. 2 | Revealing nitrogen-containing impurities in commercial metal oxides and metallic irons. a, HPLC graphs of commercial metal oxides. The retention time is 16.2 min or 18.1 min for NO_2^- or NO_3^-, respectively. **b**, Mass spectrometry curves ($m/z = 30$) for Fe_2O_3 (Alfa Aesar no. 45007) and Bi_2O_3 (Alfa Aesar no. 45582) under elevated temperature in argon showing the evolution of NO. Blank: no added sample. **c**, UV–vis spectra of the resulting solutions of various commercial irons stained with indophenol blue colourimetric reagents (Fe^{2+} was precipitated and filtered out before measurements). The peak absorbance at 660 nm was proportional to the concentration of NH_4^+, which originated from the nitrides impurities in the iron samples (Supplementary Fig. 1). The solutions were prepared by dissolving ~50 mg of the samples in 0.1 M H_2SO_4. For the Alfa Aesar-40337 sample, a twofold dilution was applied to keep the NH_4^+ concentration in the calibration range. The vendors, item numbers, lot numbers, labelled assays and values of nitrides-N content of the tested samples are summarized in Supplementary Table 2. **d**, X-ray photoelectron spectroscopy nitrogen 1s profiles of commercial iron.

402.5–403.5 eV) on the surface of a nitrided iron on exposure to oxygen[30]. Due to the very high content of nitrogen impurities in Alfa Aesar-40337, a discernible nitrogen signal was even shown in the SEM–EDS analysis (Supplementary Fig. 3).

A case analysis on the H_2O–NaOH–KOH system

Based on the above findings, we have carefully examined the H_2O–NaOH–KOH system previously reported[19] to reduce N_2 to NH_3 catalysed by nanoscale Fe_2O_3 in an undivided cell (Supplementary Figs. 4–7). We first conducted the electrolysis in a H_2O–NaOH–KOH electrolyte containing 40 wt% of water and equal moles of NaOH and KOH (denoted as 40% H_2O–NaOH–KOH hereafter) at 200 °C, loaded with Fe_2O_3 (Alfa Aesar no. 45007) catalyst. Under a constant applied current of 250 mA, the total catalyst mass-normalized NH_3 production was 39.2 ± 1.3 μmol NH_3 g_{cat}^{-1}, which is very close to the content of NO_3^- impurities in Alfa Aesar-45007 determined by HPLC (563 ± 21 ppm-N, equivalent to 40.2 ± 1.5 μmol-N g_{cat}^{-1}), corresponding to a total nitrogen match of 97.5% on average (Fig. 3a and Supplementary Fig. 5). Similarly, ~100% nitrogen balance was also obtained using the other seven NO_x^--containing metal oxides under the same conditions, except for Bi_2O_3 (Alfa Aesar no. 45582) due to the competition between Bi_2O_3 reduction and NO_x^- reduction.

We also performed longer-term measurements using $^{15}N_2$ with a closed-loop gas circulation system (Supplementary Fig. 4). To reevaluate the NRR in the H_2O–NaOH–KOH electrolyte as described in ref. [19], the H_2O–NaOH–KOH electrolyte with minimum water content (also referred to as molten NaOH–KOH) was used here. With $^{14}N_2$ or $^{15}N_2$ being circulated in the system, two conditions were tested: (1) 1 g of metallic iron (Sigma-Aldrich no. 255637) without electrolytic current for 12 h; and (2) electrolysis at 20, 100, 250, 500, 1,000 mA (2.5 h for each current) with 5 g of Fe_2O_3-washed. Only $^{14}NH_4^+$ was detected for both $^{15}N_2$ circulating experiments, and the cumulative $^{14}NH_3$ generations fell in the range of the background signal (Fig. 3b). The results of both ^{15}N-labelling experiments and the accurate balance of elemental nitrogen are highly consistent with the discovery of nitrogen impurities in the catalysts and collectively suggest that the true source of the electrochemically produced NH_3 should be reassigned from gaseous N_2 to the nitrogen-containing impurities in the Fe_2O_3 catalyst.

Recommendation on screening NO_x^-/nitrides impurities in catalyst materials

The substantial levels of NO_x^-/nitrides impurities in the commercial catalysts are surprising. It is worth noting that researchers

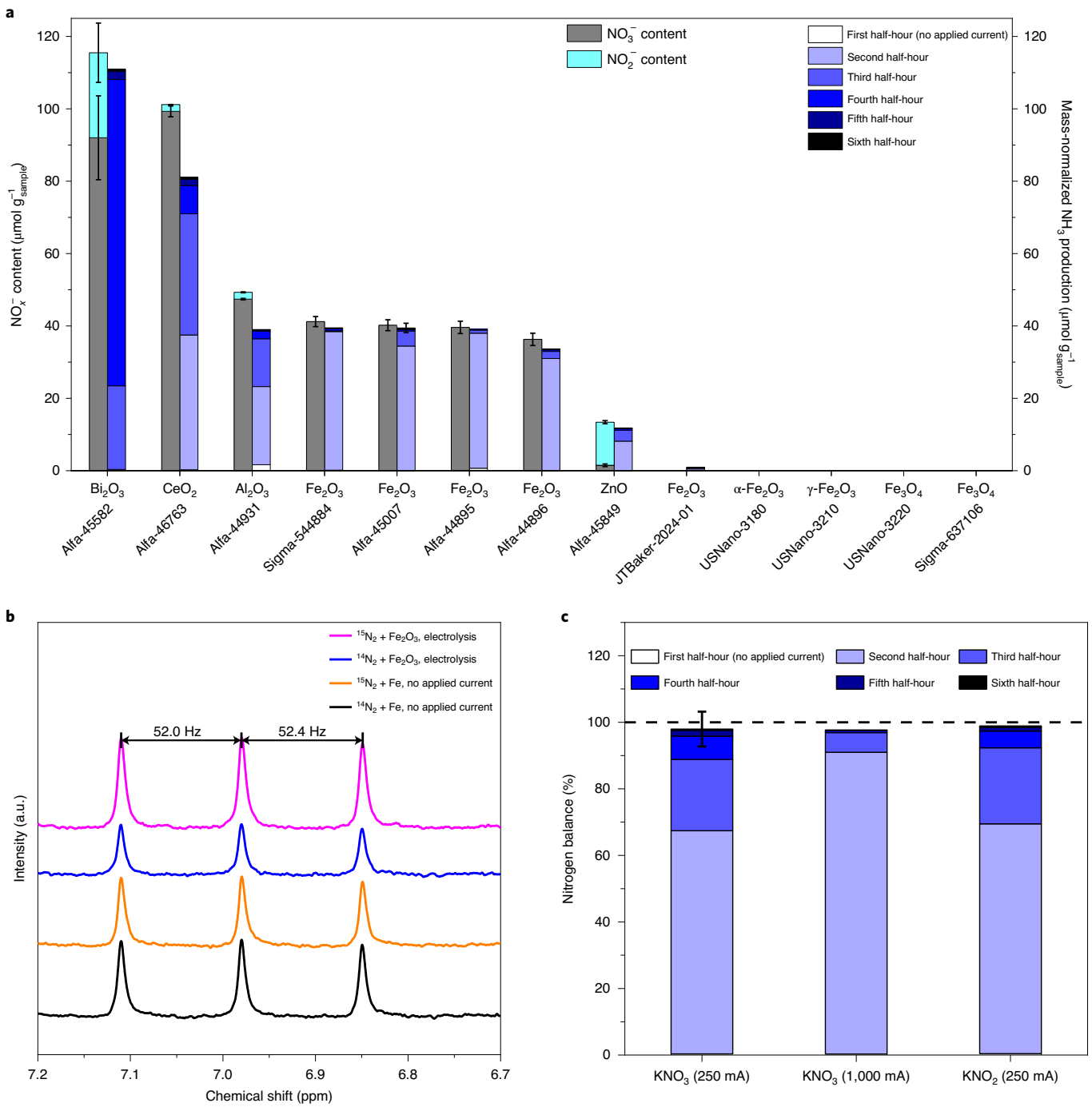

Fig. 3 | Electrolysis in the H_2O–NaOH–KOH systems. a, A comparison between the determined NO_x^- contents by HPLC (left columns) and the observed (catalyst) mass-normalized NH_3 production (right columns, divided into half-hour periods) during electrolysis for commercial oxides. The error bars represent the standard deviation of NO_x^- content, or total NH_3 production from Fe_2O_3 (Alfa Aesar no. 45007) for six independent tests (Supplementary Fig. 5). Such a comparison signifies the nitrogen-element balance. The first half-hour corresponds to the initial period of gas purging with no applied current, and electrolysis was performed in the subsequent half-hour periods until the NH_3 generation became negligible. The applied current was 250 mA for all cases except for Bi_2O_3 (where the current was 1,000 mA due to the competition between Bi_2O_3 reduction and NO_x^- reduction). The nitrogen balance reached ~100% for most cases within the first hour of electrolysis. **b**, NMR spectra (2,048 scans) of trapping solutions that contain NH_4^+ produced in longer-term N_2 circulation experiments in the molten NaOH–KOH electrolyte. Only $^{14}NH_4^+$ (triplet peaks) was detected for both $^{15}N_2$ circulating experiments, with no identifiable $^{15}NH_4^+$ signal (doublet peaks if existing). The cumulative $^{14}NH_3$ generations fell in the range of the background signal. **c**, Nitrogen balance for electrolysis at different currents with 20 mg of standard KNO_3 or KNO_2 in 40% H_2O–NaOH–KOH. The error bar represents the standard deviation of nitrogen balance for three independent electrochemical tests with KNO_3 at 250 mA.

in the long history of nitrogen fixation were periodically perplexed and impacted by the issues that arise from nitrogen contamination[11,32]. The observed NO_x^-/nitrides impurities in commercial metal oxides/metallic irons provide another account of impurity identification, on top of nitrogen-containing contaminations observed in various experimental materials

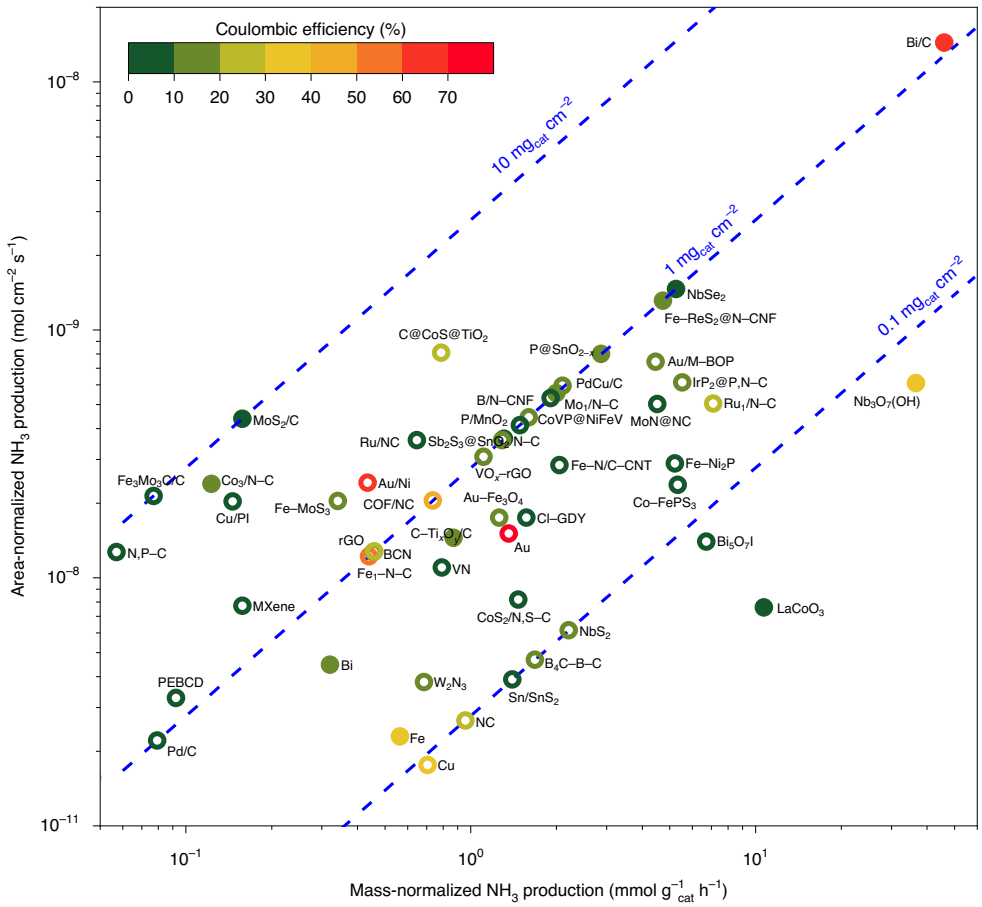

Fig. 4 | Area- and mass-normalized NH_3 production of reported NRR electrocatalysts. Each dashed line represents a constant catalyst loading in the electrolytic cell. The electrode area typically ranges from 0.25 to 1 cm^2. All data points are subject to the control experiment with $^{15}N_2$-isotopic labelling: either quantitative control (filled circles) or qualitative control (open circles). The NH_3 production rates, Coulombic efficiencies and other information are from the literature and summarized in Supplementary Table 3. rGO, reduced graphene oxide; PEBCD, poly(*N*-ethyl-benzene-1,2,4,5-tetracarboxylic diimide); GDY, graphdiyne; CNT, carbon nanotube.

including electrolytes[33], membranes[34], feeding gases[35] and even nitrile gloves[12].

In light of this discovery, we call attention to the necessity to screen the NO_x^-/nitrides impurities in commercial materials before employing them for future evaluation in NH_3 electrosynthesis, as the nitrogen-containing impurities are commonly not listed in vendors's assay documents. Laboratory-made catalysts might also be subject to NO_x^-/nitrides impurities screening when nitrogen-containing materials are involved in catalyst preparation and handling. And a simple two-step procedure (alkaline treatment for NO_x^- or acidic treatment for nitrides, followed by either HPLC or UV–vis analysis) is thereby recommended as a reliable protocol for researchers, as the procedure has been proven to be highly effective in quantifying the level of NO_x^-/nitrides impurities in metal oxides and metallic irons. Note that using deionized water instead of the alkaline solution to treat the catalysts in the first step of the procedure resulted only in partial extraction of NO_x^- (Supplementary Fig. 2).

We also suggest the reporting of (catalyst) mass-normalized NH_3 production, in addition to the area-normalized NH_3 production for future research. Figure 4 compares the mass- and area-normalized NH_3 production from catalysts reported in NH_3 electrosynthesis. The area-normalized NH_3 production ranges across three orders of magnitude (from 2×10^{-11} to 2×10^{-8} mol cm^{-2} s^{-1}), as does the mass-normalized NH_3 production (from 0.05 to 50 mmol g^{-1} h^{-1}); however, the area-normalized NH_3 production does not always align with the mass-normalized NH_3 production. One could be cautious to the catalyst with high area-normalized NH_3 production yet low mass-normalized one. Furthermore, reporting mass-normalized NH_3 production might help compare N_2 fixation across different approaches (Supplementary Fig. 8) to reasonably locate and evaluate the catalytic activity of a system.

Conclusions

Substantial levels of NO_3^--N and nitrides-N were unexpectedly revealed from some commercial metal oxides (for example, 563 ± 21 ppm-N in Alfa Aesar-45007) and metallic irons (for example, 7,297 ± 99 ppm-N in Alfa Aesar-40337), respectively. A simple two-step procedure (alkaline treatment for NO_x^- or acidic treatment for nitrides, followed by either HPLC or UV–vis analysis) is recommended as a reliable protocol for screening NO_x^-/nitrides impurities in catalyst materials. We also suggest reporting both (catalyst) mass-normalized and (electrode) area-normalized NH_3 production in future research. With both ^{15}N-labelling experiments and the accurate balance of elemental nitrogen, the true source of the electrochemically produced NH_3 in the electrolysis with the H_2O–NaOH–KOH system was correctly reassigned from gaseous N_2 to the nitrogen-containing impurities in those catalysts. Our findings on the considerable levels of nitrogen-containing impurities in many commercial metal oxides in the present Analysis are to serve the nitrogen-fixation community in a positive manner by raising awareness of the presence of high-level nitrogen-containing impurities in some commercial materials so as to avoid the misinterpretation (in the early research stage) of synthesized NH_3 originating from N_2 rather than from NO_x^--based impurities.

Although ineffective at reducing N_2 (as shown in the preceding results), the H_2O–NaOH–KOH system exhibited the efficacy to reduce NO_x^- to NH_3 with ~100% selectivity (Fig. 3c). Conceptually, an alternative route can be constructed by coupling NO_x^- reduction and direct oxidation of N_2 with O_2—the latter process could be achieved at low energy consumption and high efficiency, especially via non-thermal plasma, as discussed in a review article by Chen and colleagues[6]. Compared with the established route[36] of $N_2 \rightarrow Li_3N \rightarrow NH_3$, the route $N_2 \rightarrow NO_x^- \rightarrow NH_3$ does not involve the use and regeneration of flammable lithium metal. As a possible candidate for NH_3 electrosynthesis, the potential merit of such route warrants future research in both technical advancement and economic evaluation. Further exploration of facile biological, biochemical, chemical, photochemical and electrochemical oxidation of N_2 to NO_x^- may open up additional productive pathways to the low carbon-footprint production of NH_3 from air and water.

Methods

Quantification of NO_3^- and NO_2^- in commercial metal oxides. A sample (500 mg) was accurately weighed and mixed with 30 ml of 0.1 M KOH (≥85 wt% of KOH and water as the remnant, Sigma-Aldrich no. 221473) solution. The sample was dispersed in the KOH solution by 30 min of ultrasonication, followed by centrifugation at 8,500 r.p.m. for 10 min. The solid was then filtered out of the KOH solution with a surfactant-free cellulose acetate filter (Corning, 0.20 μm of pore size). After extraction, the NO_x^- in the resulting solution was then analysed by HPLC[37] (Agilent Technologies, 260 Infinity II LC System) equipped with a variable wavelength detector (Agilent 1260 Infinity Variable Wavelength Detector VL). The wavelength of 213 nm was chosen for NO_x^- detection. A C18 HPLC column (Gemini 3 μm, 110 Å, 100 × 3 mm) was used for analysis at 25 °C with a binary gradient pumping method to drive mobile phase at 0.4 ml min^{-1}. The mobile phase consisted of 0.01 M *n*-octylamine (99+%, Acros Organics) in a mixed solution containing 30 vol% methanol (HPLC grade, Fisher Chemical) and 70 vol% deionized water (18.2 MΩ cm, Barnstead E-Pure), and the pH of the mobile phase was adjusted to 7.0 with phosphoric acid (85%, Fisher Chemical). The running time was kept at 30 min for every sample and the retention time for NO_3^- and NO_2^- was around 18 and 16 min, respectively. The calibration solutions for NO_3^- or NO_2^- were prepared with KNO_3 (≥99.0%, Fisher Chemical) or KNO_2 (97%, Acros Organics), respectively, in the concentration range of 0.0625–2 mM (Supplementary Fig. 1).

Determination of nitrogen content in commercial iron. Specifically, ~50 mg of the commercial iron sample was accurately weighed and charged into 100 ml of 0.1 M H_2SO_4 (TraceMetal Grade, Fisher Chemical) for complete dissolution. For the Alfa Aesar-40337 sample, a twofold dilution was applied to keep the NH_4^+ concentration in the calibration range. The concentration of NH_4^+ in the solution was determined by the colourimetric method (detailed below) after removing the iron ions by precipitation with 200 μl of 6 M NaOH (≥98%, Sigma-Aldrich no. S5881) solution followed by filtration. The low-solubility product (K_{sp}) values[38] for $Fe(OH)_2$ (4.87×10^{-17}) and $Fe(OH)_3$ (2.79×10^{-39}) ensured both Fe^{2+} and Fe^{3+} can be effectively removed at pH 13 (the final pH of the solution before the colourimetric test). NMR measurement (detailed below) was also carried out for the Fe^{2+}-containing sample solution (Supplementary Fig. 3).

Colourimetric quantification of NH_3. Ammonia in 0.1 M H_2SO_4 was quantified by the well-established method with indophenol blue colourimetry. Four reagents were freshly prepared, including (1) colouring solution, containing 0.4 M sodium salicylate (≥99.5%, Sigma-Aldrich) and 0.32 M NaOH; (2) oxidizing solution, containing 0.75 M NaOH in NaClO solution (available chlorine: 4.00–4.99%, Sigma-Aldrich); (3) catalyst solution, containing 10 mg ml^{-1} of $Na_2[Fe(CN)_5NO]\cdot 2H_2O$ (≥99%, Sigma-Aldrich); and (4) 6 M NaOH solution. Specifically, 200 μl of 6 M NaOH solution was added into 4 ml of the testing sample. Afterwards, 50 μl of the oxidizing solution, 500 μl of the colouring solution, and 50 μl of the catalyst solution were added sequentially, followed by ultrasonication for 10 s to mix the reagents. The absorbance measurement was performed on a UV–vis spectrophotometer (Shimadzu UV-2700) at a wavelength of 660 nm after 2 h of colour development. The calibration curve (Supplementary Fig. 1) was established by examining a series of standard NH_3 solutions (prepared based on the Hach standard solutions) from 100 ± 2 mg l^{-1} as NH_3-N to 0–2.5 mg l^{-1} (in N) with 0.1 M H_2SO_4. The sample solution was diluted with 0.1 M H_2SO_4 if its NH_4^+ concentration is out of the calibration range. An ammonia test kit (API) was used to quickly estimate the NH_4^+ level and determine the dilution factor.

NMR quantification of $^{14}NH_4^+$ and $^{15}NH_4^+$. ^{1}H-NMR spectra were obtained on an NMR spectrometer (Bruker Avance NEO 400 MHz system). The NMR sample was prepared by mixing 800 μl of the sample solution containing NH_4^+ (in 0.1 M H_2SO_4 medium) with 200 μl of DMSO-d_6 (99.9% D, Cambridge Isotope Laboratories, Inc.)[36]. The standard $^{14}NH_4^+$ (prepared based on NH_3 solutions from Hach) and $^{15}NH_4$ solutions (prepared based on $^{15}NH_4Cl$, ≥98 at% ^{15}N, Sigma-Aldrich) were utilized for calibration with concentrations ranging from 0.1 to 5 mg l^{-1} (in ^{14}N and ^{15}N). Water suppression was carried out for all NMR measurements. The scan number was chosen to be 1,024 for 1–5 mg l^{-1} and 2,048 for lower concentrations. The NMR calibration curves are shown in Supplementary Figs. 3 and 6.

Determination of hydrazine. N_2H_4 contents were measured by the Watt and Chrisp method[39]. The colouring solution consisted of 2.0 g of *p*-dimethylaminobenzaldehyde (Fisher Chemical) in 10 ml of hydrochloric acid (TraceMetal Grade, Fisher Chemical) and 100 ml of ethanol (200 Proof, Decon). Specifically, 5 ml of the sample was mixed with 5 ml of colouring solution. After 15 min, absorbance measurement was performed on the UV–vis Spectrophotometer at the wavelength of 458 nm. Calibration solutions were prepared by dissolving $N_2H_4\cdot 2HCl$ (99%, Acros Organics) in 0.1 M H_2SO_4 to 0–2 mg l^{-1} (in N) (Supplementary Fig. 1).

Material characterization. X-ray photoelectron spectroscopy was performed on a Kratos Amicus/ESCA 3400 X-ray photoelectron spectrometer with a magnesium K-alpha X-ray (1,253.7 eV), and all spectra were calibrated with the carbon 1*s* peak at 284.8 eV. For the nitrogen 1*s* region, the scan number was increased to obtain distinguishable signals. SEM-EDS was performed on a field-emission scanning electron microscope (FEI Quanta-250) equipped with a light-element X-ray detector and an Oxford Aztec energy-dispersive X-ray analysis system. Samples were directly loaded onto the carbon tapes without applying conductive coatings. TGA–MS measurements were carried out on a Netzsch STA 449 F1 Jupiter simultaneous thermal analyser with a mass spectrometer to determine the evolved gases. Samples were loaded in alumina crucibles, and the ramping rate was applied at 10 °C min^{-1} from room temperature to 250 °C, followed by an isothermal step at 250 °C for 1 h. The measurements were carried out under flowing argon (99.999%, Airgas) at a constant flow rate of 30 ml min^{-1}.

Removal of NO_3^- in Fe_2O_3 (Alfa Aesar no. 45007). The NO_3^- in commercial Fe_2O_3 can be removed by an alkaline washing or heat treatment. Specifically, for alkaline washing, 6 g of the Fe_2O_3 sample was dispersed in 1 l of 0.1 M KOH solution by ultrasonication for 30 min, followed by vacuum filtration and finally by washing with 2 l of deionized water until pH of the filtrate reaches 7. After drying under vacuum for 12 h, the NO_3^--removed Fe_2O_3 sample by alkaline washing was obtained and labelled as Fe_2O_3-washed. For heat treatment, the Fe_2O_3 powder was heated in an oven at 180 °C for 12 h. The obtained NO_3^--removed Fe_2O_3 sample by heat treatment was denoted as Fe_2O_3-HT.

Electrolyte preparation and cell operation. We conducted the electrolysis in a H_2O–NaOH–KOH electrolyte containing 40 wt% or 9.3 wt% of water and equal moles (0.73 mol each) of NaOH and KOH at 200 °C. Note that the 9.3% H_2O–NaOH–KOH (that is, molten NaOH–KOH) was prepared by mixing commercial NaOH and KOH without adding any extra water, and its 9.3 wt% of water content was solely from the KOH chemical (containing 15 wt% of water). In a typical test, the catalyst powder was charged and dispersed into the electrolyte to form a suspension. Ultrahigh-purity N_2 or argon (99.999%, Airgas) at the flow rate of 100 ml min^{-1} was bubbled throughout the test. The exhaust gas from the electrolytic cell was bubbled into a 0.1 M H_2SO_4 trapping solution (100 ml) for NH_4^+ quantification. A constant current (typically, 250 mA) between the electrodes was applied by a potentiostat (WaveDriver 20 Bipotentiostat/Galvanostat) after 30 min of gas bubbling (the first half-hour). During electrolysis, the trapping solution was changed every half hour for NH_4^+ quantification until no considerable NH_3 production can be detected. Photographs of the entire set-up and cell components are shown in Supplementary Fig. 4.

Data availability

Source data are provided with this paper. All data supporting the findings of this study are available from the corresponding author on reasonable request.

Received: 14 April 2020; Accepted: 21 September 2020;
Published online: 26 October 2020

References

1. Apodaca, L. E. *Nitrogen (Fixed)—Ammonia. U.S. Geological Survey, Mineral Commodity Summaries* (2020).
2. Nørskov, J., Chen, J., Miranda, R., Fitzsimmons, T. & Stack, R. *Sustainable Ammonia Synthesis—Exploring the Scientific Challenges Associated with Discovering Alternative, Sustainable Processes for Ammonia Production* (US DOE Office of Science, 2016).
3. Wang, L. et al. Greening ammonia toward the solar ammonia refinery. *Joule* **2**, 1055–1074 (2018).
4. Foster, S. L. et al. Catalysts for nitrogen reduction to ammonia. *Nat. Catal.* **1**, 490–500 (2018).

5. Soloveichik, G. Electrochemical synthesis of ammonia as a potential alternative to the Haber–Bosch process. *Nat. Catal.* **2**, 377–380 (2019).
6. Chen, J. G. et al. Beyond fossil fuel-driven nitrogen transformations. *Science* **360**, eaar6611 (2018).
7. Martín, A. J., Shinagawa, T. & Pérez-Ramírez, J. Electrocatalytic reduction of nitrogen: from Haber–Bosch to ammonia artificial leaf. *Chem* **5**, 263–283 (2019).
8. Tang, C. & Qiao, S.-Z. How to explore ambient electrocatalytic nitrogen reduction reliably and insightfully. *Chem. Soc. Rev.* **48**, 3166–3180 (2019).
9. Shipman, M. A. & Symes, M. D. Recent progress towards the electrosynthesis of ammonia from sustainable resources. *Catal. Today* **286**, 57–68 (2017).
10. Greenlee, L. F., Renner, J. N. & Foster, S. L. The use of controls for consistent and accurate measurements of electrocatalytic ammonia synthesis from dinitrogen. *ACS Catal.* **8**, 7820–7827 (2018).
11. Suryanto, B. H. R. et al. Challenges and prospects in the catalysis of electroreduction of nitrogen to ammonia. *Nat. Catal.* **2**, 290–296 (2019).
12. Andersen, S. Z. et al. A rigorous electrochemical ammonia synthesis protocol with quantitative isotope measurements. *Nature* **570**, 504–508 (2019).
13. Du, H.-L., Gengenbach, T. R., Hodgetts, R., MacFarlane, D. R. & Simonov, A. N. Critical assessment of the electrocatalytic activity of vanadium and niobium nitrides toward dinitrogen reduction to ammonia. *ACS Sustain. Chem. Eng.* **7**, 6839–6850 (2019).
14. Hu, B., Hu, M., Seefeldt, L. & Liu, T. L. Electrochemical dinitrogen reduction to ammonia by Mo_2N: catalysis or decomposition? *ACS Energy Lett.* **4**, 1053–1054 (2019).
15. Zhao, Y. et al. Ammonia detection methods in photocatalytic and electrocatalytic experiments: how to improve the reliability of NH_3 production rates? *Adv. Sci.* **6**, 1802109 (2019).
16. Manjunatha, R., Karajić, A., Teller, H., Nicoara, K. & Schechter, A. Electrochemical and chemical instability of vanadium nitride in the synthesis of ammonia directly from nitrogen. *ChemCatChem* **12**, 438–443 (2020).
17. Wang, Y. et al. Generating defect-rich bismuth for enhancing the rate of nitrogen electroreduction to ammonia. *Angew. Chem. Int. Ed.* **58**, 9464–9469 (2019).
18. Lv, C. et al. An amorphous noble-metal-free electrocatalyst that enables nitrogen fixation under ambient conditions. *Angew. Chem. Int. Ed.* **57**, 6073–6076 (2018).
19. Licht, S. et al. Ammonia synthesis by N_2 and steam electrolysis in molten hydroxide suspensions of nanoscale Fe_2O_3. *Science* **345**, 637–640 (2014).
20. Zhou, F. et al. Electro-synthesis of ammonia from nitrogen at ambient temperature and pressure in ionic liquids. *Energy Environ. Sci.* **10**, 2516–2520 (2017).
21. Hu, L. et al. Ambient electrochemical ammonia synthesis with high selectivity on Fe/Fe oxide catalyst. *ACS Catal.* **8**, 9312–9319 (2018).
22. Furuya, N. & Yoshiba, H. Electroreduction of nitrogen to ammonia on gas-diffusion electrodes loaded with inorganic catalyst. *J. Electroanal. Chem. Interfacial Electrochem.* **291**, 269–272 (1990).
23. Gadalla, A. M. & Yu, H. F. Thermal decomposition of Fe(III) nitrate and its aerosol. *J. Mater. Res.* **5**, 1233–1236 (1990).
24. Kodama, H. Synthesis of a new compound, $Bi_5O_7NO_3$, by thermal decomposition. *J. Solid State Chem.* **112**, 27–30 (1994).
25. Sarkas, H., Murray, P., Fay, A. & Brotzman, R. Nanocrystalline mixed metal oxides—novel oxygen storage materials. *MRS Proc.* **788**, L4.8 (2011).
26. Birkeland, K. On the oxidation of atmospheric nitrogen in electric arcs. *Trans. Faraday Soc.* **2**, 98–116 (1906).
27. Smil, V. *Enriching the Earth: Fritz Haber, Carl Bosch, and the Transformation of World Food Production* 62–64 (MIT Press, 2004).
28. Verdouw, H., Van Echteld, C. J. A. & Dekkers, E. M. J. Ammonia determination based on indophenol formation with sodium salicylate. *Water Res.* **12**, 399–402 (1978).
29. Ertl, G., Huber, M. & Thiele, N. Formation and decomposition of nitrides on iron surfaces. *Z. fur Naturforsch. A* **34**, 30–39 (1979).
30. Torres, J., Perry, C. C., Bransfield, S. J. & Fairbrother, D. H. Low-temperature oxidation of nitrided iron surfaces. *J. Phys. Chem. B* **107**, 5558–5567 (2003).
31. Baltrusaitis, J., Jayaweera, P. M. & Grassian, V. H. XPS study of nitrogen dioxide adsorption on metal oxide particle surfaces under different environmental conditions. *Phys. Chem. Chem. Phys.* **11**, 8295–8305 (2009).
32. Davies, J. A., Boucher, D. L. & Edwards, J. G. The question of artificial photosynthesis of ammonia on heterogeneous catalysts. *Adv. Photochem.* **19**, 235–310 (1995).
33. Li, L., Tang, C., Yao, D., Zheng, Y. & Qiao, S.-Z. Electrochemical nitrogen reduction: identification and elimination of contamination in electrolyte. *ACS Energy Lett.* **4**, 2111–2116 (2019).
34. Nash, J. et al. Electrochemical nitrogen reduction reaction on noble metal catalysts in proton and hydroxide exchange membrane electrolyzers. *J. Electrochem. Soc.* **164**, F1712–F1716 (2017).
35. Dabundo, R. et al. The contamination of commercial $^{15}N_2$ gas stocks with ^{15}N–labeled nitrate and ammonium and consequences for nitrogen fixation measurements. *PLoS One* **9**, e110335 (2014).
36. Kim, K., Chen, Y., Han, J.-I., Yoon, H. C. & Li, W. Lithium-mediated ammonia synthesis from water and nitrogen: a membrane-free approach enabled by an immiscible aqueous/organic hybrid electrolyte system. *Green. Chem.* **21**, 3839–3845 (2019).
37. Chou, S.-S., Chung, J.-C., And, D.-F. & Hwang, D.-F. A high performance liquid chromatography method for determining nitrate and nitrite levels in vegetables. *J. Food Drug Anal.* **11**, 11 (2003).
38. Haynes, W. M. *CRC Handbook of Chemistry and Physics* (CRC, 2016).
39. Watt, G. W. & Chrisp, J. D. Spectrophotometric method for determination of hydrazine. *Anal. Chem.* **24**, 2006–2008 (1952).

Acknowledgements

This research was partly supported by ARPA-E agency through REFUEL program (grant no. DE-AR0000812) and by Iowa Economic Development Authority (IEDA, grant no. AWD-019199). We are grateful to S. D. Cady, D. Jing, and B. W. Boote from Iowa State University for their generous assistance in NMR and material characterization. We also acknowledge fruitful discussions with J. Li, E. A. Smith, H. Lin, B. H. Shanks, R. C. Brown, J. L. Trettin (Iowa State University), K. Kim (University of Illinois at Urbana-Champaign) and G. Soloveichik (ARPA-E) on the electrosynthesis of ammonia. W. Li thanks his Bailey Research Career Development Award and Richard Seagrave Professorship. Y. Chen acknowledges his Catron Graduate Fellowship from Catron Center for Solar Energy Research at Iowa State University.

Author contributions

W.L., S.G. and S.L. proposed the research and supervised the project. Y.C. performed material characterization. H.L. carried out HPLC measurements. Y.C. and N.H. set up the electrolytic cell system with the assistance from S.G. and S.L. and performed the electrochemical studies. Y.C., S.G., S.L. and W.L. co-wrote the paper. All authors discussed the results and commented on the manuscript.

Competing interests

The authors declare no competing interests.

Additional information

Supplementary information is available for this paper at https://doi.org/10.1038/s41929-020-00527-4.

Correspondence and requests for materials should be addressed to S.L., S.G. or W.L.

Reprints and permissions information is available at www.nature.com/reprints.

Publisher's note Springer Nature remains neutral with regard to jurisdictional claims in published maps and institutional affiliations.